EVALUATION OF ALTITUDE CONTROL FOR AN AIRBREATHING HYPERSONIC AIRCRAFT MODEL

Masaharu Hiruma*
***The University of Tokyo, PO Box 113-8656, 7-3-1 Hongoh Bunkyo-ku, Tokyo, Japan**

Keywords: *HST, PID, CFD, Waverider*

Abstract

The objective of this paper is to evaluate the flight trajectory of the Airbreathing Hypersonic Experimental Aircraft Model. For the evaluation, the flight trajectory with the smallest fuel consumption over downrange ratio was analysed through parametric study with the flight path angle γ being the parametric variable. The Airbreathing Hypersonic Experimental Aircraft model was constructed using CFD and a surrogate model was created to interpolate the coefficients to the aircraft dynamics. A benchmark PID controller was constructed with the angle of attack and thrust being the control input to the aircraft model. From the results, the flight path angle of -4deg had the smallest fuel consumption over downrange ratio while flight path angle of -10deg exceeded the load factor constraint.

1 Introduction

In recent years, the demand for commercial flight has seen increased over the years and 20 years into the future, the number is expected to double [1]. To meet the expectations of the rising demand for intercontinental travel, Japan Aerospace Exploration Agency (JAXA) is currently researching a hypersonic transport (HST) aircraft in pursuit for faster and reliable flight system [2]. The aircraft is planned to be equipped with a hypersonic pre-cooled turbo jet engine (PCTJ) under development and its target speed region ranges from take-off to Mach 5 [2].

In order to make hypersonic flight of practical use, JAXA has set a road map for the demonstration of a hypersonic transport (Fig.1).

Fig. 1. Hypersonic Flight Experiment Overview

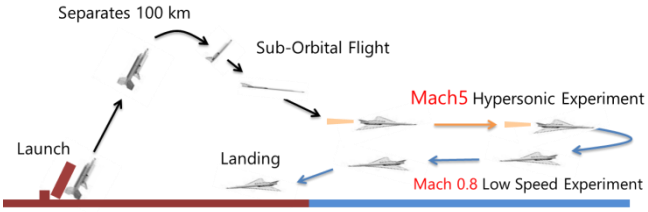

Fig. 2. Flight Profile of Second Stage

The road map is broken into 3 stages. The 1st stage is the High Mach Integrated Control Experiment (HIMICO) and its experiment objective is to test engine and aircraft system under real environment. 2nd stage is the Hypersonic Cruise Experimental Aircraft (HyCruise) and its experiment objective is to test hypersonic cruise and low speed flight capability. Two 3 m PCTJ engines are placed on both sides of the fuselage each producing 1 kN of thrust. The aircraft will be attached to the fuselage of the NAL735 booster rocket. It will reach 100 km altitude and will drop into the atmosphere. By use of suborbital flight, the aircraft will accelerate until 50 kPa of dynamic pressure is met. Then, the aircraft will perform a pull up maneuver and will begin its engine test at a speed of Mach 5[2)] (Fig.2). After the hypersonic experiment has been conducted, the aircraft will turn around to perform a low speed flight test and land to the designated airstrip. The 3rd stage is the

Hypersonic Business Jet and its objective is to test for practical use.

In order to increase valid test duration, airframe design with high lift to drag ratio (L/D) increases range as can be seen from the Breguet Range Equation (1).

$$Range = U \times \frac{L}{D} \times I_{sp} \times ln\left(\frac{W_i}{W_f}\right) \qquad (1)$$

Where U = cruise velocity (m/s), L = lift (N) D = drag (N), I_{sp} = Specific Impulse, W_i and W_f = initial and final weight of the aircraft. From an aerodynamic viewpoint, increasing the L/D is essential but attaining it in the hypersonic speed regime has been proven to be difficult with the "L/D barrier" by Kuchemann [3]. In this present work a high L/D is considered a benchmark in aerodynamic efficiency and attaining it becomes an important factor. For this, an airframe concept known as a waverider outputs high L/D by utilizing the high pressure on its lower surface produced by its own shock wave along its leading edge [3].

In this work, a new model of an Airbreathing Hypersonic Aircraft (Fig. 3) has been constructed with a waverider applied as its wing (waverider wing) which utilizes the high L/D during hypersonic cruise. Specifications are shown in Table 1. The waverider wing is defined as a wing which utilizes the shock wave attached to its leading edge forming a compressed lower surface thus increasing L/D. The waverider wing is depicted in Fig. 4. The method for deriving the waverider wing can be found in [4]. Previous studies conducted so far through the use of Computational Fluid Dynamics (CFD) validate the aerodynamic efficiency and the results suggest a relatively high L/D at their given design conditions [4]. The model has been evaluated at low speed of Mach 0.3 where CFD results stated sufficient lift was produced for low speed flight [5].

This experimental aircraft aims to conduct a hypersonic cruise experiment at Mach 5. Therefore, a waverider was applied as the wing of the aircraft in order increase L/D during hypersonic cruise. Also, this aircraft will conduct a low speed cruise experiment at Mach 0.8 to evaluate the subsonic performance

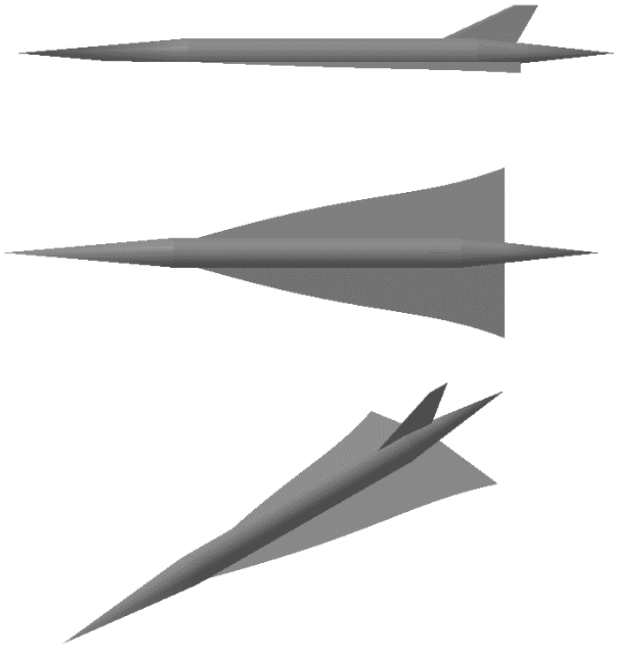

Fig. 3. Airbreathing Hypersonic Aircraft

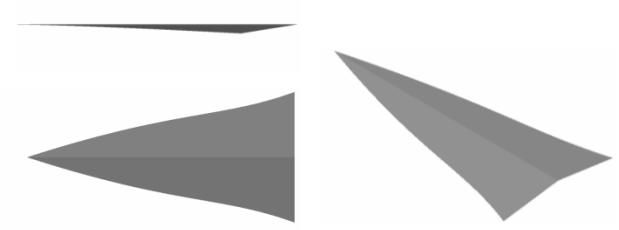

Fig. 4. Waverider Wing

Table 1. Waverider Model Specifications

Total Length [m]	9.6
Total Weight [kg]	803
Wing Span [m]	3.2
Mean Aerodynamic Chord [m]	3.7
Fuselage Radius [m]	240
Projected Area [m^2]	8.3
Volume [m^3]	1.02
C.G. (from nose)	60%

of the engine and the aerodynamics.

Although many CFD has been conducted for the evaluation of cruise and low speed flight [4][5], simulation of actual flight trajectory has not been conducted. The aircraft model is still in need of thorough validation of its aerodynamics, however a preliminary test on flight control is needed since control in hypersonic speed may prove difficult. The difficulty in control is closely related to the constraints placed on the flight trajectory in terms of fuel consumption and

descent downrange. Although the total amount of fuel needed has not been decided, limiting the fuel consumption is critical since liquid hydrogen is used for fuel. Liquid hydrogen has a very high specific energy (MJ/kg) however, a very low energy density (MJ/L). This makes it hard to store large quantity of liquid hydrogen in fuel tanks and fuel shortage may occur [6]. Limiting the downrange is critical as well since from the flight profile (Fig.2), the aircraft will turn around and land to the designated airstrip. From this, the descent downrange should be kept minimal so as to minimize the total distance needed to cover for the return flight. Therefore, evaluation on the trajectory minimizing the fuel consumption over downrange ratio is necessary in the preliminary analysis of the flight trajectory.

2 Research Objective

The objective of this paper is to construct a benchmark PID controller satisfying the constraints placed on the flight trajectory as well as to evaluate the flight trajectory of the Airbreathing Hypersonic Experimental Aircraft Model (obtained through CFD) with the smallest fuel consumption over downrange ratio. This was evaluated through parametric study with the γ being the parametric variable.

3 Aerodynamic and Engine Model

The aerodynamic model was derived by an unstructured three-dimensional CFD solver developed by JAXA known as FaSTAR [7] (Fast Aerodynamic Routine). A three-dimensional flow-field around the model was calculated numerically.

Numerical analysis was conducted solving the three-dimensional compressible Navier-Stokes equation using finite-volume method (Table 2). The viscous model effects were estimated using SA-noft2 [9] and HLLEW [10] scheme for advection was used to accurately capture shockwaves and discontinuities. Time integration was performed using MUSCL [11] method with second-order spatial accuracy.

The calculated Mach numbers are shown in Table 3. The total length of the aircraft was used as the reference length.

Table 2. Numerical Analysis Conditions

Governing equation	Navier-Stokes
Turbulence model	SA-noft2 [9]
Numerical scheme	HLLEW [10]
Volumetric Accuracy	MUSCL, 2nd order [11]
Time Integration	LU-SGS [12]

Table3. Calculated Mach Numbers

Mach	0.3, 0.8, 2, 4, 5, 6

Table 4: Sample Points for RBFN

Mach	0.3, 0.8, 2, 4, 5, 6
AoA [deg]	-10,-8,-6,-4,-2,0,2,4,6,8,10
Altitude [km]	0~30
Thrust [kN]	0~6

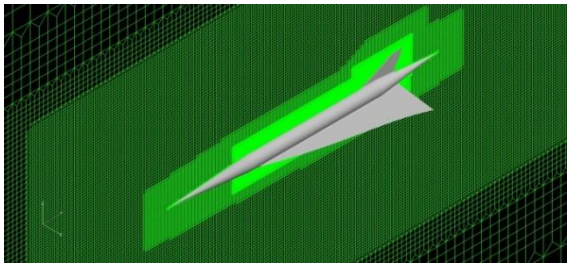

Fig. 5. Unstructured Mesh by Hexagrid [7]

An automatic hexahedra grid generator Hexagrid [8] developed by JAXA was used to create three-dimensional grids. Based on the input geometry (STL format), Hexagrid generates unstructured mesh based on Cartesian mesh. A grid containing approximately 40 million cells in an 81 cubic meter domain was created for each model (Fig 5).

Interpolation to the aircraft dynamics was carried out by a method known as the radial basis network (RBFN) [13]. The sample points used to generate the RBFN is summarized in Table 4. The RBFN used to interpolate the lift and drag coefficients are depicted in Fig. 6 and Fig. 7 respectively. The simulation uses U.S. Standard Atmosphere Model for the air density and static temperature [14]. Lastly, thrust is defined as T (N) and has a maximum output of 1600 N at Mach5 and 2000N at below Mach0.8 which was derived from the data provided by JAXA at Mach 0.8. Interpolation of I_{sp} was made using RBFN as a function of thrust and altitude (Fig. 8).

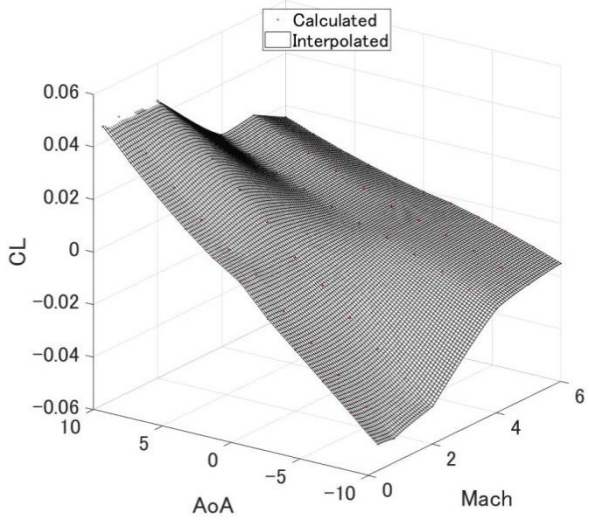

Fig. 6. C_L Interpolation Surface Curve

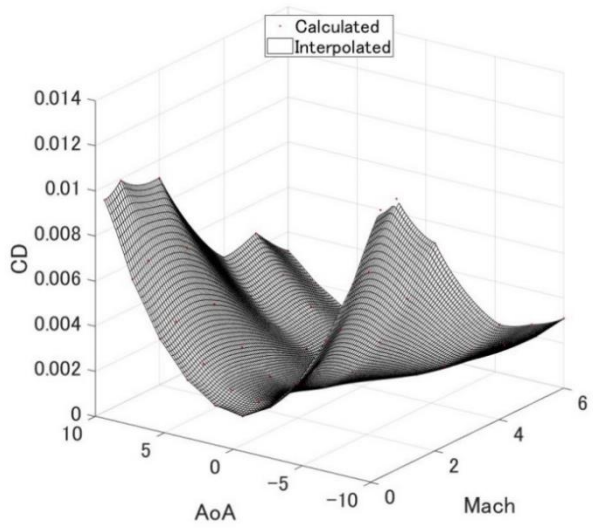

Fig. 7. C_D Interpolation Surface Curve

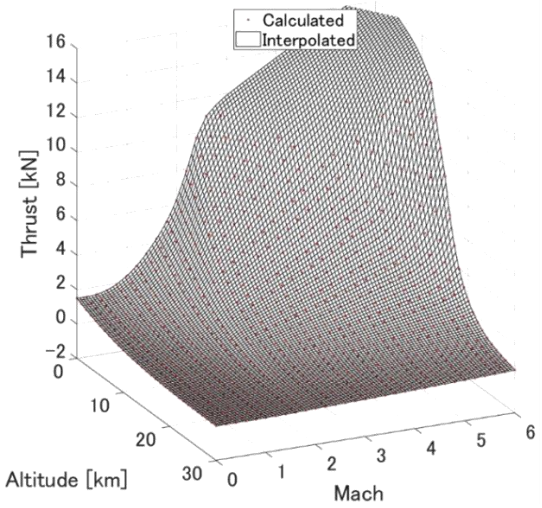

Fig. 8. Thrust Interpolation Surface Curve

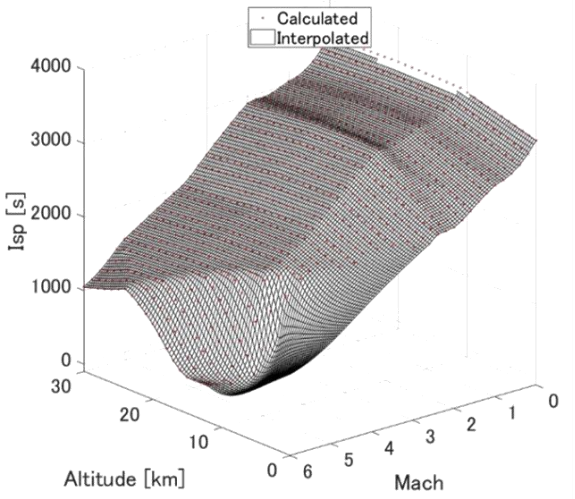

Fig. 9. I_{sp} Interpolation Surface Curve

4 Aircraft Dynamics and Variables

The longitudinal equation of motion used to define the aircraft dynamics with assumption of a round non-rotating earth as well as various variables are given by the following nonlinear equations. Where v: aircraft velocity(m/s), γ: flight path angle(deg), h: altitude(m)+radius of the earth, d : downrange(km), m :fuel consumption, T: thrust, L: lift, D:drag, F_z:load factor (G), q:dynamic pressure (kPa), m_0:aircraft weight (kg), α: angle of attack (deg), μ is the gravitational constant($3.96 \times 10^{14}\mathrm{m}^3/\mathrm{s}^2$), and r is the radius of the earth (6378145m), I_{sp}:specific impulse (s), F:thrust (N), g:9.8(m/s^2). The non-dimensional coefficients of lift C_L and drag C_D are each a function of Mach number and angle of attack obtained from CFD analysis.

$$\dot{v} = \frac{Tcos(\alpha) - D}{m_0} - \frac{\mu sin(\gamma)}{r^2} \tag{2}$$

$$\dot{\gamma} = \frac{L + Tsin(\alpha)}{m_0 v} - \frac{(\mu - v^2 r)cos(\gamma)}{vr^2} \tag{3}$$

$$\dot{h} = vsin(\gamma) \tag{4}$$

$$\dot{d} = vcos(\gamma) \tag{5}$$

$$\dot{m} = \frac{F}{I_{sp} g} \tag{6}$$

$$F_z = Lcos(\alpha) + Dsin(a) \tag{7}$$

$$q = \frac{1}{2}\rho v^2 \tag{8}$$

$$L = \frac{1}{2}\rho v^2 S C_L(Mach, \alpha) \quad (9)$$

$$D = \frac{1}{2}\rho v^2 S C_D(Mach, \alpha) \quad (10)$$

5 PID Controller

For the simulation, a longitudinal flight control system controlling the altitude was constructed (Fig.10). Here, $\gamma_{target}(t)$ represents the target flight path angle and $v_{target}(t)$ represents the target Mach number of Mach 0.8 respectively.

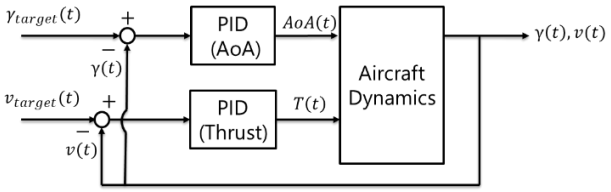

Fig. 10. Flight Control System

The two PID controllers consist of controlling the angle of attack (AoA) and Thrust relative to the deflection detected from the aircraft dynamics output of flight path angle and velocity $\gamma(t)$ and $v(t)$ respectively. The time constant for AoA and thrust was presumed to be 0.5deg/s and 6N/s respectively.

The gain parameters of the flight controller are summarised in Table 5. The proportional, integral, and derivative gains for the AoA controller are the following;$K_{pAoA}, K_{iAoA}, K_{dAoA}$. Proportional, integral, and derivative gains for the thrust controller are the following; K_{pT}, K_{iT}, K_{dT}. The parameters for the gain used in the PID controllers were set so as to have high target tracking performance. The target in this case would be the reference trajectory given by the parametric γ. The parametric γ evaluated in this research are summarised in Table 6. The gamma inputs are given as a Bessel function.

$$t^2\ddot{\gamma} + t\dot{\gamma} + (t^2 - n^2)\gamma = 0 \quad (11)$$

Where t: time (s), γ: flight path angle (deg), $n = 15$: integer order.

6 Simulation Setup

The simulation is carried out in Matlab/ Simulink environment. The simulation assumes a descent trajectory for simplicity. The initial conditions prior to starting the simulation are summarized in Table 7. The constraints are summarized in Table 8. The thrust limitation for Mach5 and Mach0.8 are taken from the PCTJ engine model provided by JAXA. The descent termination conditions are summarized in Table 9 where v (m/s) is the aircraft velocity, γ (rad) is the flight path angle, h (m) is the altitude.

Table 5. Gain Parameters

Parameters	Values
$(K_{pAoA}, K_{iAoA}, K_{dAoA})$	$(200, 0, 900$
(K_{pT}, K_{iT}, K_{dT})	$(1000, -2, 10)$

Table 6. Flight Path Angle for Parametric Study

Flight Path Angle [deg]	-2 -4 -6 -8 -10

Table 7. Initial Conditions

Altitude [km]	25
Mach	5
Trim Angle [deg]	1.4
Pitching Moment [Nm]	0
Thrust [N]	1535
Control Off : t_{off} [s]	$t_{off} \leq 500$
Control On : t_{on} [s]	$500 < t_{on} \leq 3600$

Table 8. Trajectory Constraints

Load Factor [G]	$-5.5 \leq F_z \leq 5.5$
Dynamic Pressure [kPa]	$q \leq 51$
Angle of Attack [deg]	$-10 \leq a \leq 10$
Trim Angle [deg]	Mach5 = 1.4
	Mach 0.8 = 2
Thrust [N]	Mach5 $\leq$ 1600
	Mach0.8 $\leq$ 2000

Table 9. Descent Termination Conditions

$\dot{v}, \dot{\gamma}, \dot{h}$	$\leq 1 \times 10^{-2}$
Final Velocity [Mach]	± 0.4

Table 10. Evaluation Function

$minimize = \frac{Fuel\ Consumption\ [\text{kg}]}{Downrange\ [\text{km}]}$

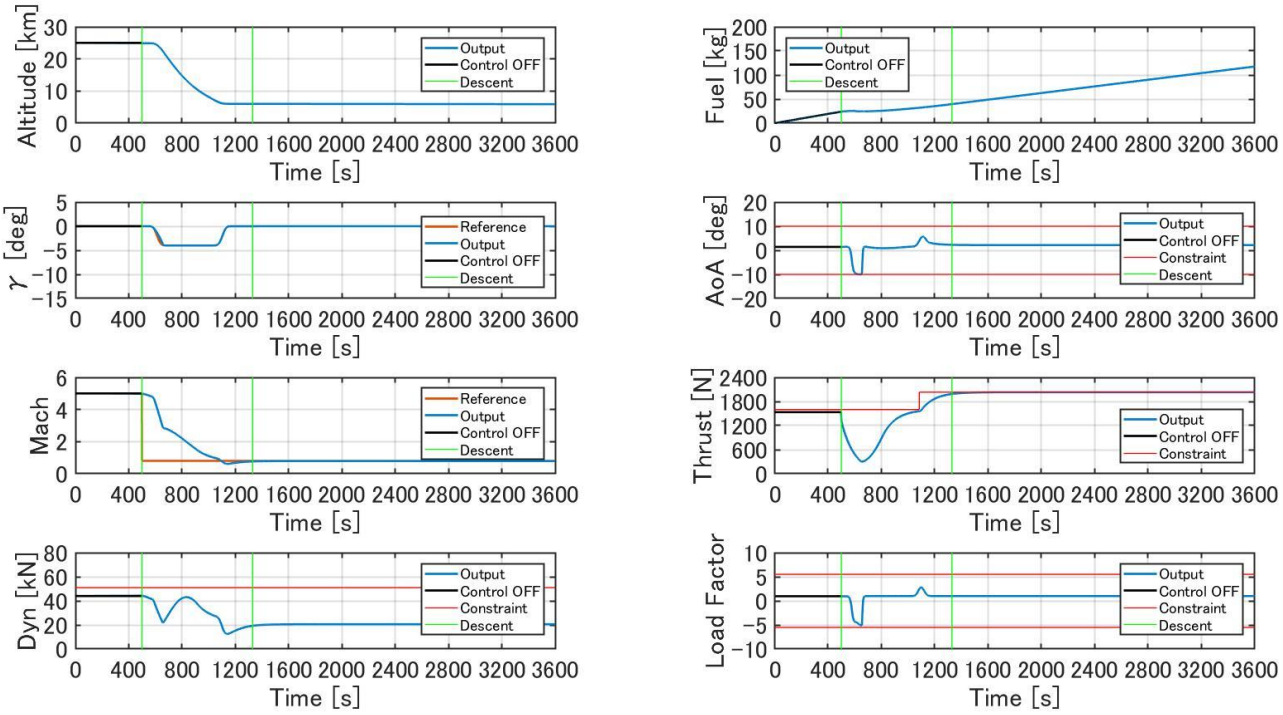

Fig. 11. Simulation Results of Flight Path Angle -4deg

The conditions for the aircraft cruising at Mach5 is trim angle of 1.4deg and the altitude 25km [5]. The target flight condition is to decrease altitude from 25km to 6km since subsonic cruise at Mach0.8 can only be sustained from this altitude. Table 10 summarizes the evaluation function. In this case, fuel consumption per unit of downrange will be minimized and evaluated.

7 Results

The simulation results are summarized in Table 11 and results for flight path angle of -4deg and -10deg are shown in Fig. 11 and Fig. 12 respectively. Fig 13 shows the downrange with respect to altitude and flight path angle with respect to fuel consumption over downrange. From Fig. 10, it can be seen that flight trajectory from the altitude of 25km to around 6km is possible with the control of AoA and thrust. However, from Fig 11, it can be seen that with γ = -10deg, the load factor constraint is violated thus the γ in which satisfies the trajectory constraints from Table 8 is up to γ= -8deg. From Fig 11 and Fig 12, it can be concluded that the simulation converges after descent maintaining cruising altitude and velocity.

Since the objective of this research is to decrease fuel consumption as much as possible while decreasing the downrange, a ratio of fuel consumption to downrange will be taken (Table 10). From Fig 12, it is evident that the evaluation function is minimized at γ = -4deg.

The simulation time for each γ decreases from 1285s to 745s as well as the downrange (Fig 13). However, the fuel consumption increases past γ = -4deg. This is due to the unwanted AoA

Table 11. Summarized Simulation Results

γ [deg]	Fuel Consumption [kg]	Downrange [km]	Descent Time [s]
-2	27.4	740	1285
-4	15.6	491	830
-6	18.1	442	830
-8	20.5	383	720
-10	17.6	365	745

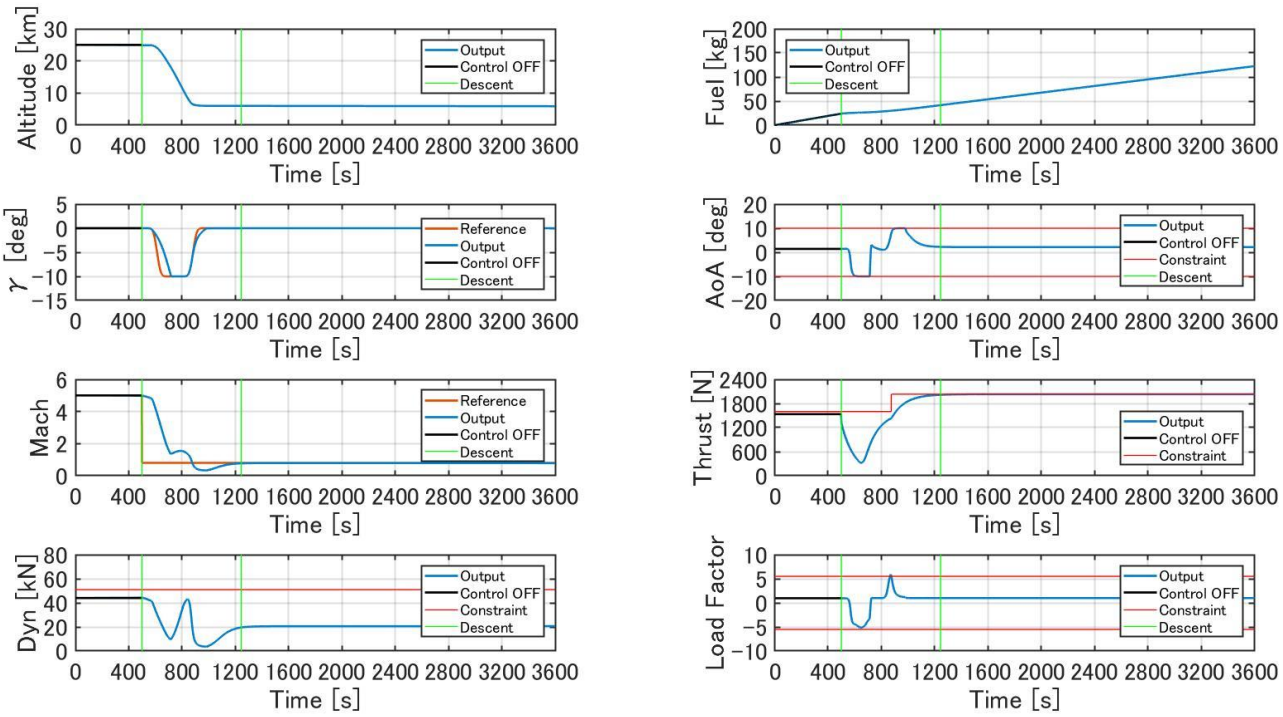

Fig. 12. Simulation Results of Flight Path Angle -10deg

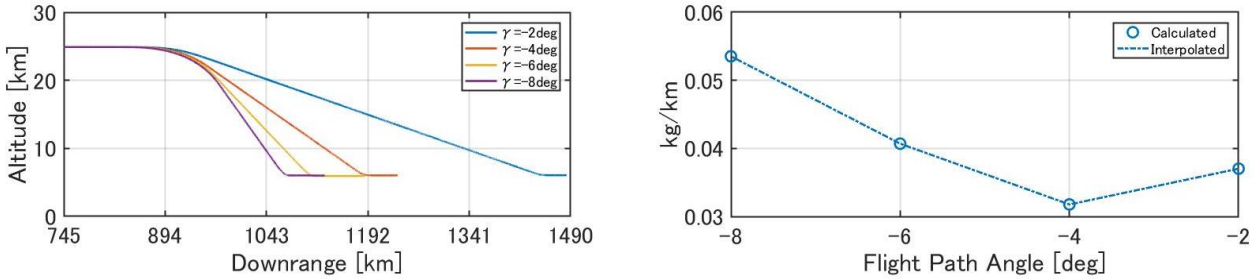

Fig. 13. Downrange to Altitude and Flight Path Angle to Fuel Consumption over downrange Comparison

gain due to aircraft pitching up. The AoA PID controller detects the γ error from the input command thus increasing the AoA created more drag. This drag creates a velocity undershoot which forces the thrust PID controller to create more thrust consuming more fuel. Reducing the velocity undershoot could decrease the fuel consumption and lower the flight path angle even further to decrease the downrange as well.

7 Conclusion

In this study, a longitudinal flight control system for altitude control was constructed and simulated for the Airbreathing Hypersonic Aircraft Model. From the simulation, the aircraft model was able to reach the target altitude and velocity with the AoA and thrust being the control input. A flight path angle minimizing fuel consumption over downrange was γ = -4deg while γ = -10deg exceeded the load factor constraint.

For future works, optimization of the PID controller is needed to reduce the undershoot caused during pitch up. Also, modelling of the elevon actuators are needed since the control delay was presumed to be 0.5deg/s. Lastly, wind tunnel experiments is needed to validate the error placed on the aerodynamic model thus opening the possibility for more robust controller such as gain scheduling.

References

[1] Japan Aerospace Exploration Agency. *JAXA2025*. Maruzen Planet Inc, 2005.

[2] Hideyuki Taguchi, Hiroaki Kobayshi, Takayuki Kojima, Motoyuki Hongoh, Tetsuya Sato, Takeshi Tsuchiya, Mitsuhiro Tsue. Flight Experiment Plan of Hypersonic Pre-Cooled Turbojet Engine. 59th Space Science and Technology Conference, Japan, 3A-11, 2015.

[3] K.G. Bowcutt, J.D. Anderson, D. Capriotti. Viscous Optimized Hypersonic Waveriders. AIAA 25th Aerospace Sciences Meeting, America, 1987.

[4] Masaharu Hiruma, Asei Tezuka, Hideyuki Taguchi, Motoyuki Hongoh. Evaluation of Waverider Derived Wing for Hypersonic Experimental Aircraft. APISAT, Australia, 2015.

[5] Masaharu Hiruma, Asei Tezuka, Hideyuki Taguchi, Motoyuki Hongoh, Tomonari Hirotani, Seigo Koga. Low Speed Aerodynamics on the Hypersonic Experimental Aircraft. 60th Space Sciences and Technology Conference, Japan, 2016.

[6] Albert M. Momenthy. Fuels of the Future. The Space Congress Proceedings, US, 1983.

[7] Atsushi Hashimoto, Takashi Ishida, Takashi Aoyama. Results of Three-Dimensional Turbulent Flow with FaSTAR, 54th AIAA Aerospace Sciences Meeting, AIAA Sci Tech Forum, AIAA 2016-1358.

[8] Hashimoto A., Murakami K., and Aoyama T.. Lift and Drag Prediction Using Automatic Hexahedra Grid Generation Method, AIAA paper 2009-1365, 2009.

[9] Aupoix, B. and Spalart, P. R.. Extensions of the Spalart-Allmaras Turbulence Model to Account for Wall Roughness, International Journal of Heat.

[10] S. Obayashi, G. P. Guruswamy. Convergence Acceleration of a Navier-Stokes Solver for Efficient Static Aeroelastic Computations, AIAA Journal Vol. 33, No.6, 1995.

[11] Van Leer, B.. Towards the Ultimate Conservative Difference Scheme, V. A Second Order Sequel to Godunov's Method, *J. Com. Phys.*., *32*, 101–136, 1979.

[12] Seokkwan Y. and Antony J.. Lower-upper Symmetric-Gauss-Seidel method for the Euler and Navier-Stokes equations, AIAA Journal, Vol. 26, No. 9, pp. 1025-1026, 1988.

[13] Forrester A.I.J, Sobester A, Keane A.J. *Engineering Design via Surrogate Modelling: A Practical Guide*. John Wiley & Sons. Chichester. 2008.

[14] U. S. Standard Atmosphere, 1976, U. S. Government Printing Office, 1976.

Contact Author Email Address

mailto: mhiruma@g.ecc.u-tokyo.ac.jp

Copyright Statement